Technical Sciences, 2022, 25, 59–75

UNIWERSYTET WARMIŃSKO-MAZURSKI W OLSZTYNIE

Yearbook peer-reviewed scientific journal
ISSN 1505-4675
e-ISSN 2083-4527
TECHNICAL SCIENCES
Homepage: https://czasopisma.uwm.edu.pl/index.php/ts/

DOI: https://doi.org/10.31648/ts.7597

OPTOELECTRONIC SYSTEM FOR CONTROLLING AN ALTERNATING CURRENT MOTOR. ELECTRICAL AND ELECTRONIC DESIGN

Zenon Syroka

ORCID: 0000-0003-3318-8495
Department of Electrical Engineering, Power Engineering, Electronics and Automatics
Faculty of Technical Sciences
University of Warmia and Mazury in Olsztyn

Received 18 March 2022, accepted 25 April 2022, available online 27 May 2022.

K e y w o r d s: digital control, motor controller, electric and hybrid vehicles, microcontroller.

A b s t r a c t

A control system for a three-phase induction motor was designed with the use of optoelectronic components and methods. Motor speed was controlled by changing supply voltage frequency. This solution ensures a wide range of rotational speeds, constant torque and effective start-up of an induction motor. The designed motor is supplied with direct current converted to three-phase alternating current. The adopted solution relies on renewable sources of energy to produce DC power. The designed electric motor is controlled by changing supply voltage frequency. Input voltage with the desired waveform is generated by the motor's electronic system that relies on two microcontrollers. The presented solution features a user interface.

Introduction

An electric motor is a machine that converts electric energy to mechanical energy. Similarly to pneumatic and hydraulic motors, electric motors have numerous technical applications. There are various types of electric motors that differ in structure and supply voltage. This study describes a control system for an electric motor.

Correspondence: Zenon Syroka, Katedra Elektrotechniki, Energetyki, Elektroniki i Automatyki, Wydział Nauk Technicznych, Uniwersytet Warmińsko-Mazurski, ul. Oczapowskiego 11, 10-719 Olsztyn, e-mail: zenon.syroka@uwm.edu.pl, syrokaz@onet.eu

The widespread use of alternating current (AC) has increased the popularity of AC motors. Unlike in most direct current (DC) motors, in AC motors, power is not supplied to the rotor via a commutator, but it is induced by the rotating magnetic field of the stator on rotor coils. The resulting voltage causes current to flow through rotor coils, and another magnetic field is generated. The magnetic field exerts torque on a current loop which moves the rotor. Alternating current motors are smaller, simpler and more compact than DC motors, but their operation is more complex to analyze. Due to the structural differences between AC and DC motors, completely different methods are also required to control the operation of AC motors.

Optoelectronics is a field of science that deals with the properties of light for advanced signal processing, including signal acquisition, transmission, conversion, accumulation and presentation. Optoelectronic solutions are widely applied in numerous industrial sectors. Optoelectronic methods are used to measure the key parameters of engine performance. Optoelectronic devices protect delicate electronic components against load shedding from mechanical parts, and they are used to display and control a system's operating parameters.

The aim of the present study was to design a control system for an AC motor with the use of optoelectronic devices and methods. The designed control system enables the user to change the motor's rotational speed and direction of shaft rotation, and it supports the visualization of the engine's operating parameters. The system facilitates the start-up of induction motors and guarantee user safety. The control system and the motor are powered by direct current, which enables the use of batteries charged from renewable energy sources.

The described solution has been patented (Syroka, Merchel 2021).

Research assumptions

The control system for an AC motor should meet the following assumptions:

– the motor should by supplied by direct current and it should enable the use of batteries for controlling mobile devices;

– the motor's rotational speed should be controlled within a wide range of values;

– the control system should minimize motor load during start-up;

– constant shaft torque should be maintained during start-up;

– the control system accessed by the user should have galvanic isolation to electronic components from high-voltage mechanical components;

– the user should be able to set the rotational speed and monitor the operation of the motor and the control system;

– the cost of the control system should be minimal.

Squirrel-cage motors supplied with three-phase alternating current are characterized by favorable operating parameters and a long service life due to their simple structure. However, DC motors require inverters that produce input voltage with the desired waveform. A three-phase bridge circuit comprising six insulated-gate bipolar transistors (IGBTs) was applied to meet this requirement. Transistors are controlled by dedicated optoelectronic drivers that rapidly reload transistor gate capacities and galvanically isolate the control system from the mechanical system. The control signal is generated by a programmed Atmel AVR microcontroller as the slave device. The control signal is generated digitally to eliminate undesirable phenomena in transistor commutation. A second microcontroller was also used as the master device to guarantee reliable generation of the control signal and to control other system functions, such as user-system communication and monitoring of engine performance. Signals are transmitted between microcontrollers by serial communication. A third microcontroller was applied as a voltmeter to measure supply voltage.

Control system operation

Motor operation was controlled by changing supply voltage frequency. This solution is optimal because it ensures a wide range of rotational speeds, constant torque and effective start-up of an induction motor. A block diagram of the control system is presented in Figure 1.

The system features a microcontroller as the master device (*1*) which is responsible for communication between the user and the system. The user can control the system via a six-key keyboard (*2*) or an infrared remote controller (*3*) using the NEC IR transmission protocol. Information is displayed on an LCD screen (*4*). The values input by the user are transmitted by the master microcontroller (*1*) to the slave microcontroller (*5*) which generates and transmits the control signal to optoelectronic drivers in IGBTs (*6*). The drivers (*6*) isolate the control system from mechanical components and protect delicate electronics against load shedding. Based on the received signal, optoelectronic drivers (*6*) activate or deactivate IGBTs (*7*) that balance voltage from the DC source (*8*). Optoelectronic drivers (*6*) are powered by a separate DC source (*9*); therefore, the failure of the main DC source (*8*) does not affect the operation of the control system. Supply voltage is measured by an electronic voltmeter (*10*), and the measured values are transmitted by the opto-isolator to the master microcontroller (*1*). Inverter supply voltage is filtered by a passive filter (*11*). The motor's rotational speed (*12*) is measured by an optoelectronic encoder (*13*) which transmits the signal to the master microcontroller (*1*). Based on the received data, the system modifies supply voltage frequency by compensating for the effects of lower DC source voltage (*8*) and motor slip (*12*). These parameters are communicated to the user on an LCD display (*4*).

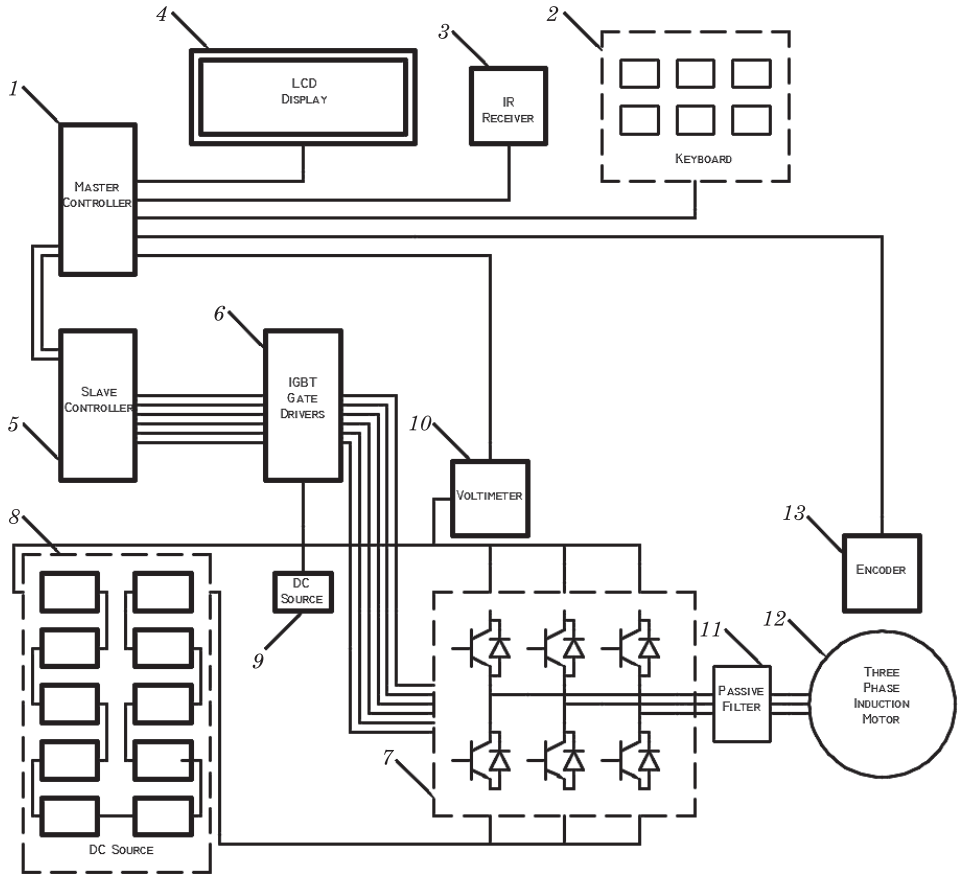

Fig. 1. Block diagram of an optoelectronic control system for a DC motor; description in the text

Master device

The master device is an ATmega 328/P microcontroller. In the designed control system for an AC motor, the master device:

– controls the user interface, i.e. a six-key keyboard (UP, DOWN, RIGHT, LEFT, ENTER, CANCEL) and an infrared remote controller using the NEC IR transmission protocol. Information is communicated to the user on the LCD display;

– controls communication between master and slave devices;

– measures the motor's rotational speed with the use of a CNY70 reflective optical sensor, a rotary encoder with an alternating black-and-white pattern, and a clock circuit in the microcontroller;

– receives voltage measurements from the voltmeter;

– monitors the operation of the control system by calculating and transmitting angular frequency values and correction factors to the slave device.

The circuit diagram of the master device is presented in Figure 2.

The voltage supplied to the microcontroller is stabilized and reduced to 5 V by the L7805CV voltage regulator. The voltage signal is taken from a 16 MHz quartz resonator. Each key in the keyboard is connected to a configured microcontroller pin, which enables the microcontroller to identify changes in their state. The keys are also connected to 0.1 μF capacitors which minimize voltage fluctuations caused by key vibrations during switching and protect the system against errors in microcontroller inputs. Current flowing through the keyboard is controlled by 470 Ohm resistors. Reverse logic was applied to the keyboard. Microcontroller pins are configured to a high logic state, and when a key is pressed, the corresponding pin switches to a low logic state. This solution minimizes the influence of external disturbances on microcontroller operation. The circuit diagram of the keyboard is presented in Figure 3.

The signal transmitted by the NEC remote control is received by the TSOP4838 receiver module, one of the three circuit clocks in the ATmega 328/P microcontroller, and a mechanism that responds to the events detected in the microcontroller's PD2 pin. The above mechanism and the NEC transmission protocol are described in the second part of the paper (software solutions). The connection diagram of the TSOP4838 receiver module is presented in Figure 4.

The receiver module is powered by a 5 V source. The 100 Ohm resistor reduces current to the required level. An additional 4.7 μF resistor minimizes fluctuations in supply voltage. The OUT pin is connected to the microcontroller's PD2 pin. A block diagram of the TSOP4838 receiver module is presented in Figure 5.

The TSOP4838 module receives the IR signal from the remote controller via a reverse-biased photodiode that blocks current. When a photon hits the diode, the generated charge carrier leads to momentary current flow. The signal is received by a preamplifier which amplifies a weak signal from the diode before it is further processed. The signal is transmitted to an automatic gain control (AGC) amplifier, and it is filtered by a band-pass filter that passes signals with a frequency of 38 Hz and rejects other signals. A demodulator recovers the signal from a modulated carrier wave and provides meaningful information for the microcontroller. The amount of amplification provided by the amplifier is determined by the amplitude of the filtered signal.

The LCD display has an internal HDD44780 controller. The controller includes a set of instructions for inputting commands and controlling the functions of the LCD display.

Master and slave microcontrollers communicate via a USART interface. RXD and TXD pins in both microcontrollers communicate in serial mode.

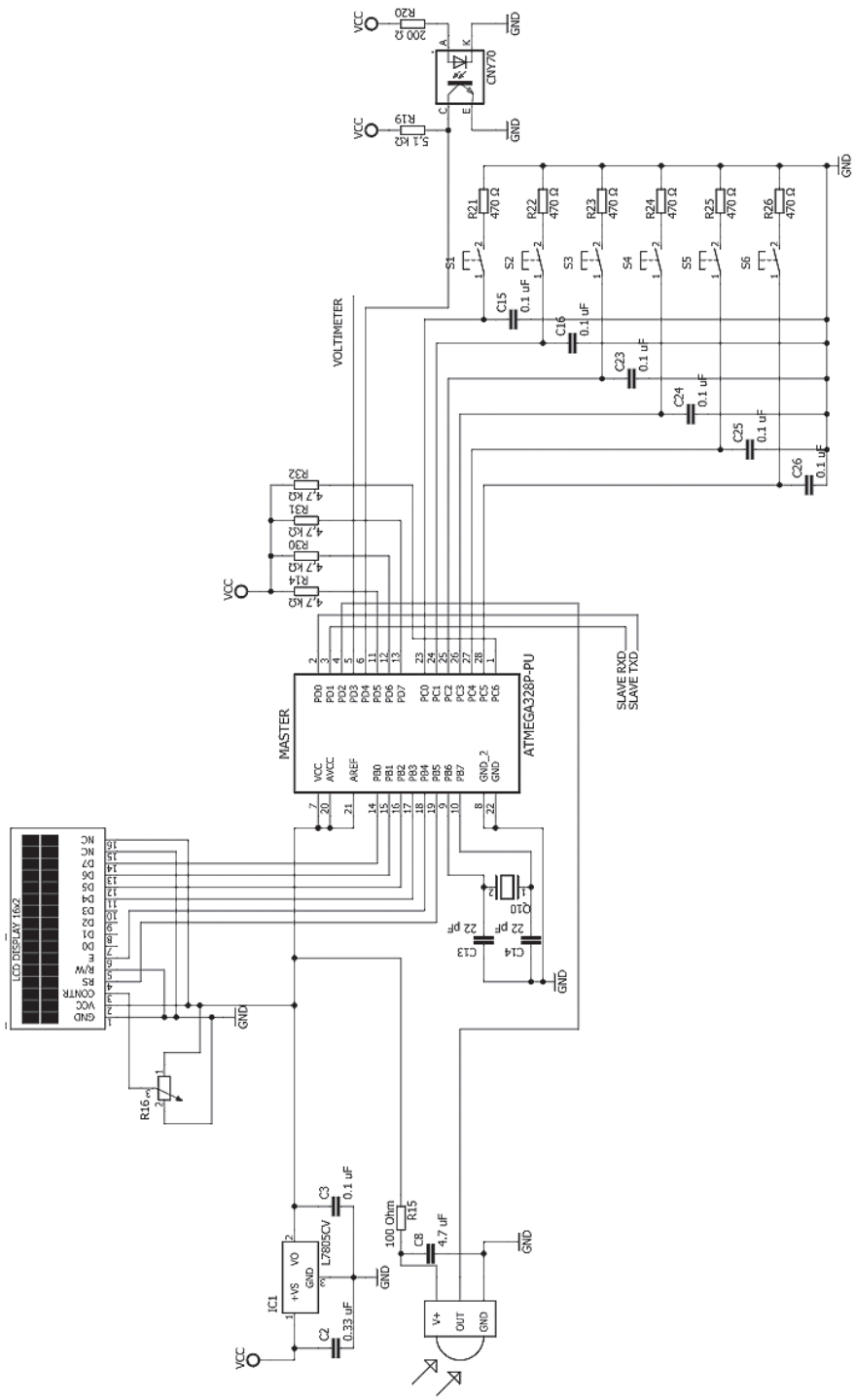

Fig. 2. Circuit diagram of the master device

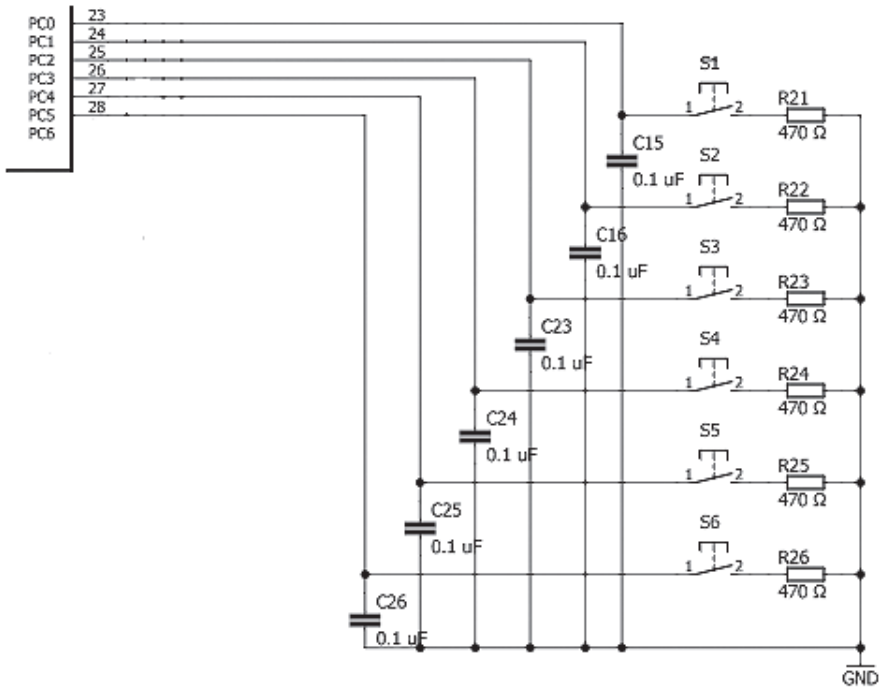

Fig. 3. Circuit diagram of the keyboard

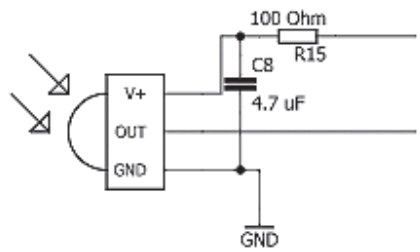

Fig. 4. Connection diagram of the TSOP4838 receiver module

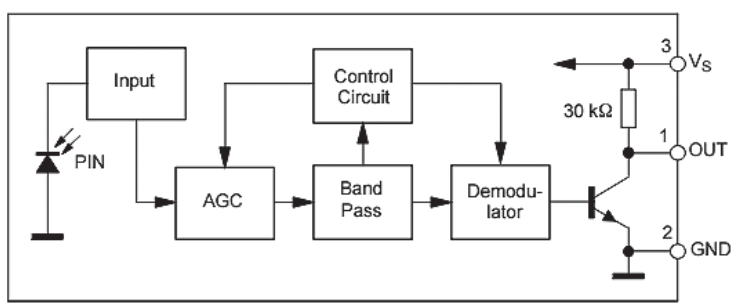

Fig. 5. Block diagram of the TSOP4838 receiver module

Four bytes are sent during each transmission: a command byte describing the task to be performed by the slave device; a data byte containing information necessary for performing the command; and command and data bytes in reverse order which are compared with the original bytes to guarantee that the transmission is reliable and to prevent the device from executing erroneous commands.

A motor's rotational speed is measured with the use of a CNY70 reflective optical sensor, a rotary encoder with an alternating black-and-white pattern, and a clock circuit in the ATmega 328/P microcontroller. The connection diagram of the CNY70 optical sensor is presented in Figure 6.

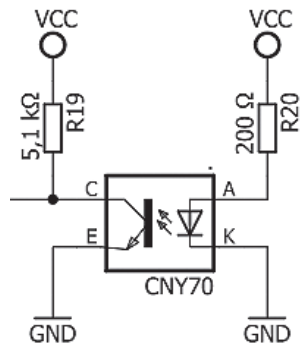

Fig. 6. Connection diagram of the CNY70 opto-isolator

The CNY70 opto-isolator comprises an LED transmitter and a phototransistor receiver. Light is absorbed when it hits the black field, the phototransistor closes, and the microcontroller pin switches to a high logic state. Light is reflected when it hits the white field, the phototransistor opens, and the pin switches to a low logic state. The motor's rotational speed can be determined by measuring the time during which pins remain in high and low state. The measured values are computed by the microcontroller and displayed on the LCD display. Unused microcontroller pins were pulled up to a high logic state to protect them against voltage disturbance.

Slave device

The slave device generates signals that control six IGBTs; therefore, six control signals have to be generated. These signals are pulse width modulation (PWM) signals that are similar to inverter output signals. In the described solution, the signals are generated by the ATmega 328/P microcontroller with three clock circuits that produce six PWM signals in six pins. The microcontroller has sufficient clock speed and memory to perform the required calculations. A circuit diagram of the slave device is presented in Figure 7.

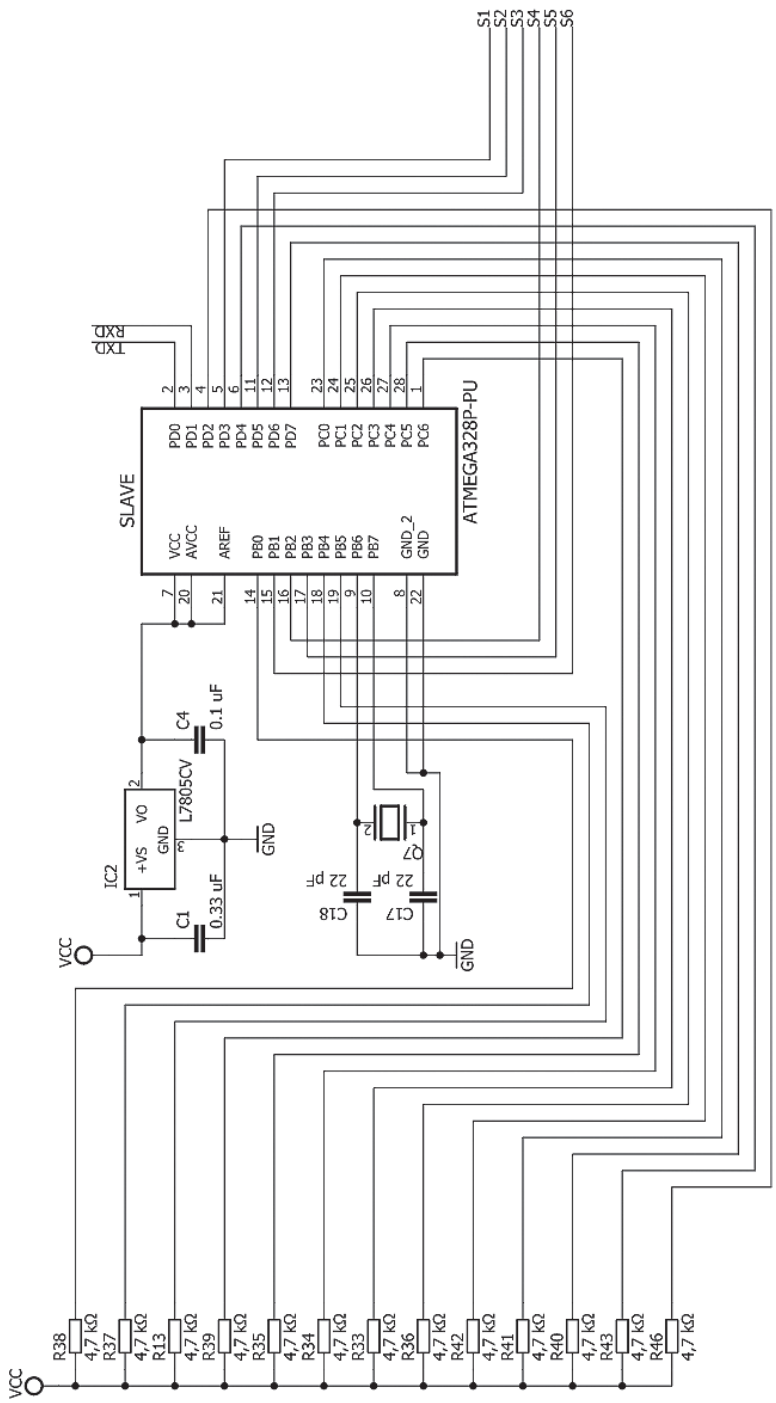

Fig. 7. Circuit diagram of the slave device

The microcontroller is powered by the L7805CV voltage regulator with an output voltage of 5 V. The voltage signal is taken from a 16 MHz quartz resonator. The control signal is generated by pins PD3, PD5, PD6, PB1, PB2 and PB3. As a result, all transistors can be controlled by a single microcontroller. Transistor pairs on the same branches are controlled by the same clock device, which eliminates switching delays caused by commutation processes. To guarantee uninterrupted operation of the control system, the slave device only generates control signals and receives commands from the master device via serial data transmission. Unused microcontroller pins were pulled up to a high logic state to protect them against voltage disturbance.

Simulink model

The control system comprises a squirrel-cage induction motor, a three-phase bridge circuit with IGBTs, a square wave generator and a three-phase sine wave reference generator for controlling the operation of the slave device, and a *Regulation* function that calculates supply voltage frequency and controls the master device. The simulation covers ten seconds of system operation with a time step of 10^{-6} seconds. A diagram of the simulation model developed in the MATLAB program is presented in Figure 8.

The motor's rotational speed was set at 20 rps during the simulation. The master device receives information about the motor's rotational speed and uses it to calculate the angular frequency of supply voltage. The master device sends a signal to the slave device which controls the three-phase bridge circuit. The bridge circuit regulates the frequency of the supply voltage reaching the motor. The simulation was conducted on the following assumptions:

– the motor is not moving when the simulation begins;

– there is no delay in IGBT switching times which are shorter than the time step in the simulation;

– constant mechanical torque of 20 N·m is applied to the motor's shaft. Torque is applied to determine slip compensation by the control system;

– simulation time is 10 s. During that time, the motor controlled by the designed system can achieve the required speed and begin stable operation.

The results of the simulation were processed in the MATLAB program to obtain the required characteristics. The following data were processed:

– motor's rotational speed [rps];
– stator phase current [A];
– electromagnetic torque [N·m];
– voltage between L1 and L2 [V];
– supply voltage frequency [Hz];
– torque compensation coefficient;
– current flow through L1 transistors [A].

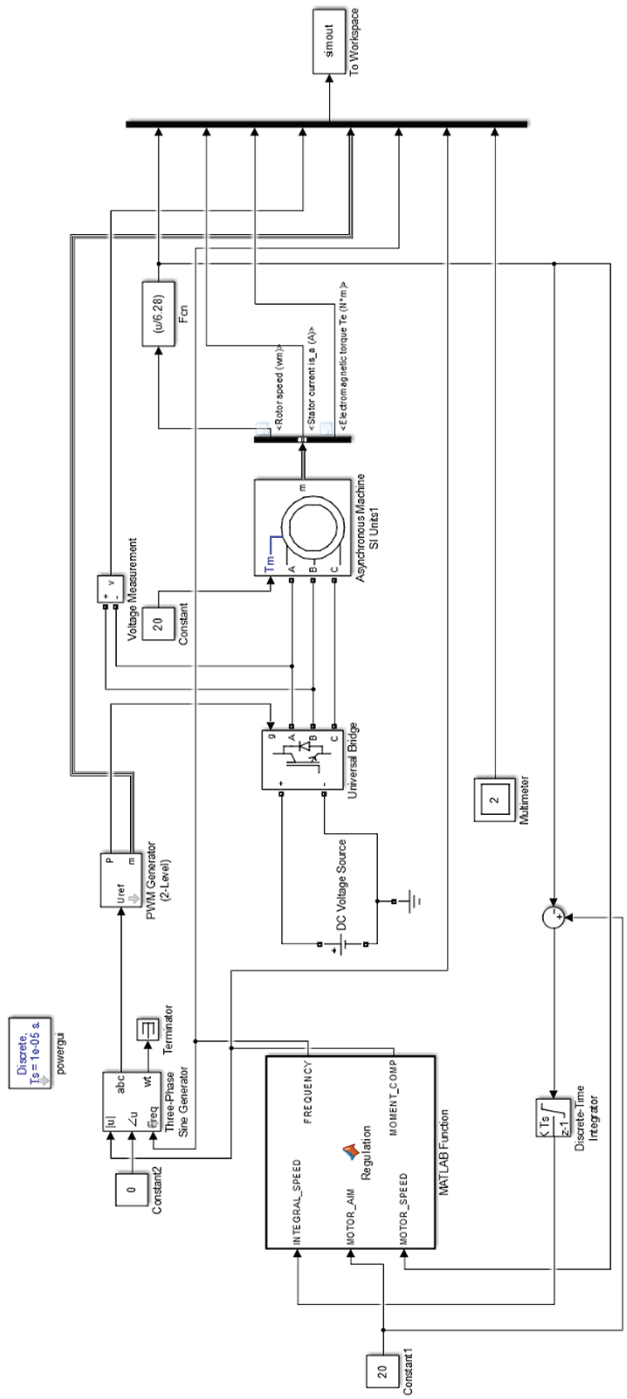

Fig. 8. Diagram of the model simulating the operation of the control system

Results

Rotational speed as a function of time is the most important characteristic from the point of view of motor control. The simulated motor speed was 20 rps. Based on the simulated speed, the master algorithm calculates subsequent values of angular frequency by comparing it with the preset value. The software of the master device featured a proportional-integral algorithm to reduce the error of the controlled variable to zero. Rotational speed as a function of time is presented in Figure 9.

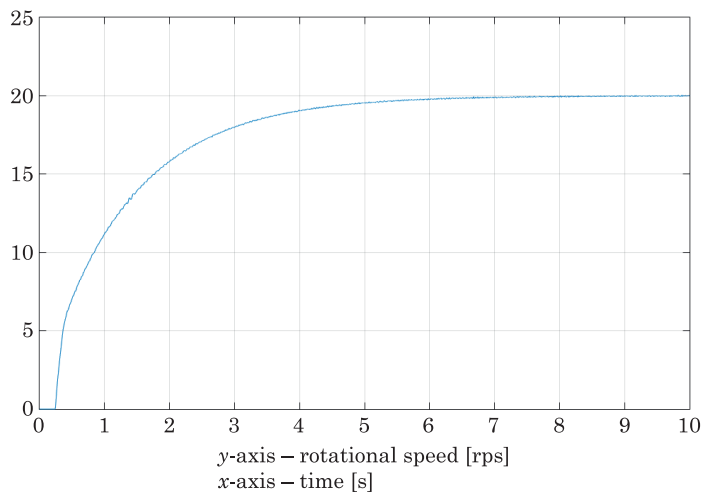

Fig. 9. Rotational speed as a function of time

Based on subsequent values of angular frequency calculated by the master device, the slave device controlling the bridge circuit generates three-phase voltage with a given frequency. The frequency of the generated voltage is presented in Figure 10.

For a four-pole motor to reach the speed of 20 rotations per second, the supplied voltage has to be twice higher than in a two-pole motor.

As demonstrated in Figure 10, motor slip increases when mechanical torque is applied to the shaft, and the frequency of supply voltage has to be increased to compensate for the above. When the preset rotational speed is achieved, the frequency of supply voltage is stabilized at 43 Hz, which is confirmed by the proportional-integral algorithm. Frequency characteristics do not deviate considerably due to low proportional gain and high integral gain. This solution increases motor stability and decreases the load resulting from the difference between the speed of magnetic field rotation and rotor speed. As a result, the time required to achieve the preset motor speed is prolonged.

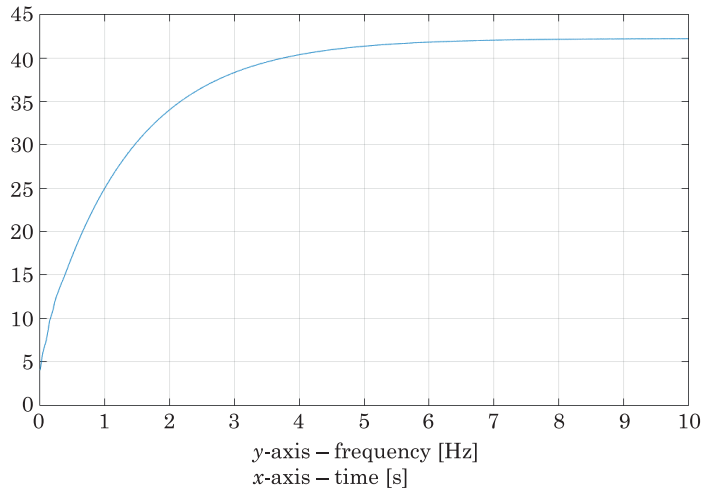

Fig. 10. Frequency of supply voltage as a function of time

The evolution of electromagnetic torque over time is yet another important parameter of motor operation (Fig. 11).

After initial fluctuations caused by the application of mechanical torque to the shaft and, consequently, prolonged motor start-up, the value of electromagnetic torque reached around 20 N·m. This value can be achieved quickly by applying the torque compensation coefficient which stabilizes the amplitude-to-frequency ratio that determines the motor's rotational speed. The evolution of the torque compensation coefficient over time is presented in Figure 12.

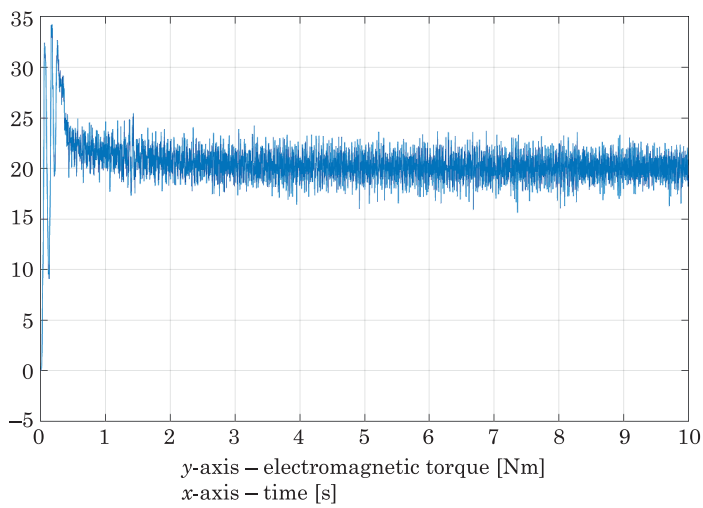

Fig. 11. Evolution of electromagnetic torque over time

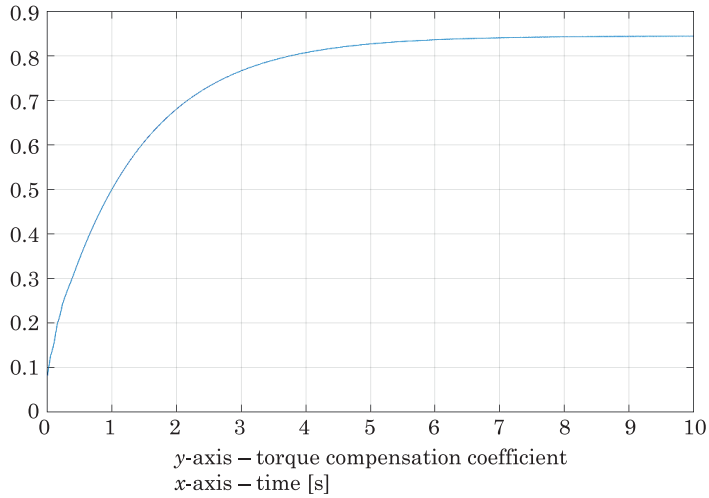

Fig. 12. Evolution of the torque compensation coefficient over time

The value of the torque compensation coefficient determines the frequency filling of current pulses and decreases supply voltage for lower frequencies. Torque is stabilized, and starting current can be decreased to protect transistors against damage. Current characteristics in transistors controlling L1 voltage presented in Figure 13.

During motor start-up, instantaneous current in IKW15T120 transistors does not exceed the preset value of 45 A, and it rapidly decreases to 30 A when the torque compensation coefficient is applied.

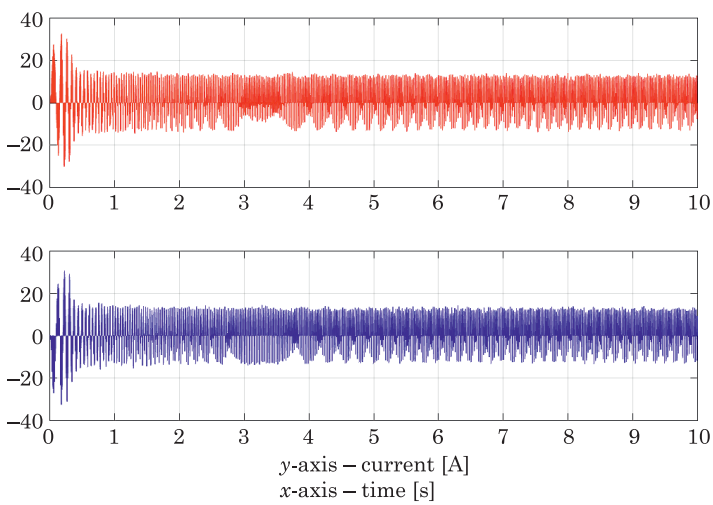

Fig. 13. Current characteristics in top and bottom L1 transistors

The pulse width modulation method generates higher voltage harmonics which exert a negative effect on motor performance. The harmonic components of voltage were determined by Fourier transform, where every periodic time function can be represented as an infinite sum of sine and cosine waves whose frequency is a multiple of the base frequency.

The voltage between L1 and L2 and stator voltage were analyzed during stable operation of an induction motor. The amplitude and frequency characteristics of interphase voltage are presented in Figure 14.

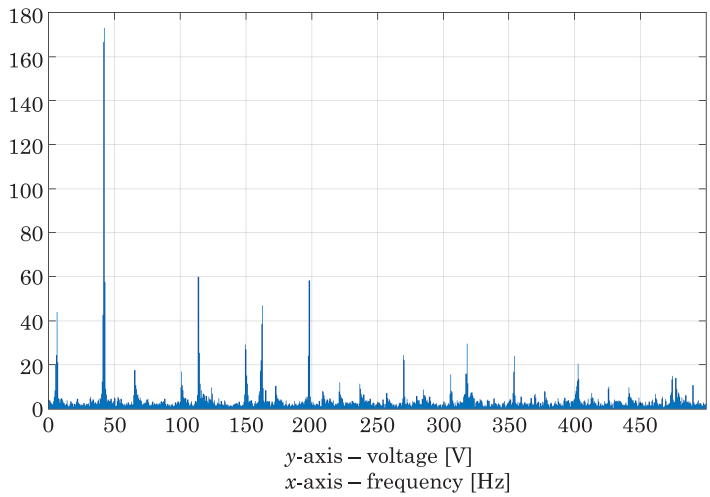

Fig. 14. Amplitude and frequency characteristics of voltage between L1 and L2

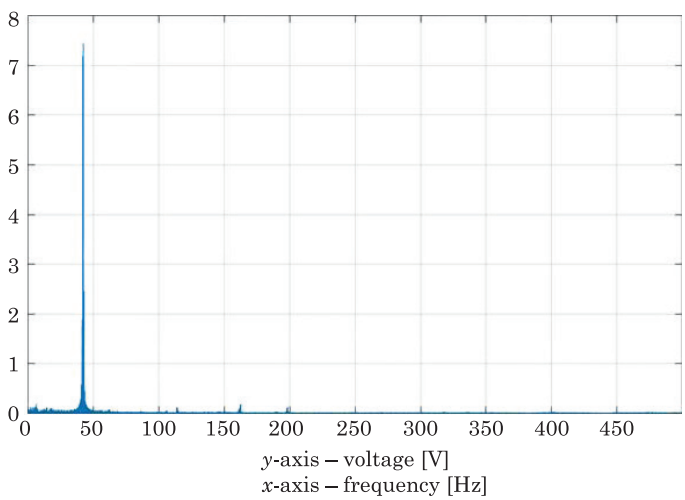

Fig. 15. Amplitude and frequency characteristics of stator current

The presence of higher harmonics in voltage supplied to the induction motor is confirmed in Figure 14. The predominant voltage frequency is the frequency set by the control system, but higher frequencies can destabilize motor performance. An analysis of Figure 15 indicates that higher harmonics are eliminated in stator current because high-frequency oscillations are damped by the induction motor. Undesirable current components can be eliminated with the use of filters. The motor's parameters have to be defined to guarantee that undesirable components are effectively filtered out.

Conclusions

An optoelectronic system for controlling an AC motor was designed. The procedure of controlling an induction motor's rotational speed and electromagnetic torque was described. The frequency of supply voltage was modified to control the motor's rotational speed within a wide range of values.

The designed electronic system comprising IKW15T120 IGBTs with a three-phase bridge circuit was patented. The control system is isolated from mechanical components with the use of VO3120 LED optoelectronic drivers that control IGBTs. The control system is based on two ATmega 328/P microcontrollers. The user interface comprises a keyboard and an IR remote controller. System information is communicated to the user via an LCD display.

The motor's rotational speed is measured by a rotary encoder and a CNY70 reflective optical sensor. Supply voltage is measured by a voltmeter based on the ATtiny13 microcontroller, and the measured values are transmitted by the opto-isolator to the master microcontroller. Based on the received values, a proportional-integral algorithm controls supply voltage frequency, and the preset rotational speed is achieved within the range of values calculated by the system.

The presented simulation confirmed that the control system compensates for motor slip by increasing supply voltage frequency. The selected parameters reduce motor load during start-up by decreasing the difference between the speed of magnetic field rotation and rotor speed. The simulation confirmed the presence of higher harmonics in supply voltage. The influence of higher harmonics can be eliminated with the use of low-pass filters.

Systems that control rotational speed by changing supply voltage frequency are increasingly applied in industrial processes because they expand the range of applications of asynchronous squirrel-cage motors. Squirrel-cage induction motors have a simple structure and a long service life, and they are gradually replacing DC motors. The designed control system can be used when an induction motor is supplied with direct current only, for example from batteries, to increase user safety and expand the motor's life expectancy.

References

ALI E., KHALIGH A., NIE Z., LEE Y.J. 2009. *Integrated Power Electronic Converters and Digital Control*. CRC Press, Boca Raton.

BOLTON W. 2006. *Programmable Logic Controllers*. Elsevier, Amsterdam, Boston.

BUSO S., MATTAVELLI P. 2006. *Digital Control in Power Electronics*. Morgan & Claypool Publisher, San Rafael, CA.

CHEN C.-T. 1991. *Analog and Digital Control system Design: Transfer Function, State Space, and Algebraic Methods*. Saunders College Publishing, Filadelfia, Pensylwania.

DENTON T. 2016. *Electric and Hybrid Vehicles*. Routledge, San Diego.

DORF R.C., BISHOP R.H. 2008. *Modern Control System Solution Manual*. Prentice Hall, New Jersey.

FADALI S. 2009. *Digital Control Engineering, Analysis and Design*. Elsevier, Burlington.

FEUER A., GOODWIN G.C. 1996. *Sampling in Digital Signal Processing and Control*. Brikhauser, Boston.

GABOR R., KOWOL M., KOŁODZIEJ J., KMIECIK S., MYNAREK P. 2019. *Switchable reluctance motor, especially for the bicycle*. Patent No. 231882.

GLINKA T., FRĘCHOWICZ A. 2007. *Brushless DC motor speed control system*. Patent No. P195447.

GREGORY P. 2006. *Starr Introduction to Applied Digital Control*. Gregory P. Starr, New Mexico.

HUSAIN I. 2003. *Electric and Hybrid Vehicles, Design Fundamentals*. CRC Press LLC, Boca Raton, London.

JONGSEONG J., WONTAE J. 2019. *Method of controlling constant current of brushless dc motor and controller of brushless dc motor using the same*. United States Patent Application Publication, US2018323736 (A1).

KHAJEPOUR A., FALLAH S., GOODARZI A. 2014. *Electric and Hybrid Vehicles Technologies, Modeling and Control: a Mechatronic Approach*. John Wiley & Sons Ltd., Chichester.

KOJIMA N., ANNAKA T. 2019. *Motor control apparatus and motor unit*. United States Patent Application Publication, US2019047517 (A1).

KOLANO K. 2020. *Method for measuring the angular position of the shaft of a brushless DC motor with shaft position sensors*. Patent No. P235653.

LANDAU I.D., ZITO G. 2006. *Digital Control Systems Design, Identification and Implementation*. Springer, London.

LUECKE J. 2005. *Analog and Digital Circuits for Electronic Control System Applications Using the TI MSP430 Microcontroller*. Elsvier, Amsterdam, Boston.

MI CH., MASRUR M.A., GAO D.W. 2011. *Hybrid Electric Vehicles Principles and Applications with Practical Perspectives*. John Wiley & Sons Ltd., Chichester.

MOUDGALYA K.M. 2007. *Digital Control*. John Wiley & Sons Ltd., Chichester.

MURRAY R.M., LI Z., SHANKAR SASTRY S. 1994. *A Mathematical Introduction to Robotic Manipulation*. CRC Press, Berkeley.

OGATA K. 1995. *Discrete Time Control Systems*. Prentice-Hall, New Jersey.

PISTOIA G. 2010. *Electric and Hybrid Vehicles Power Sources, Models, Sustainability, Infrastructure and the Market*. Elsevier, Amsterdam, Boston.

SIKORA A., ZIELONKA A. 2011. *Power supply system for a BLDC motor*. Patent No. P.394971.

SOYLU S. 2011. *Electric Vehicles – the Benefits and Barriers*. Edited by Seref Soylu, Rijeka.

STEVIĆ Z. 2013. *New Generation of Electric Yehicles*. Edited by Zoran Stević, Rijeka.

SYROKA Z.W. 2019. *Electric Vehicels – Digital Control*. Scholars' Press, Mauritius.

SYROKA Z.W., JAKOCIUK D. 2020. *Battery recharging system in electric vehicle*. Patent No. P431380, filing date: 17 January 2020.

SYROKA Z.W., MERCHEL D. 2021. *Optoelectronic control system for an alternating current motor*. Patent decision of 5 February 2021; patent No. PL 236459.

ŚLUSAREK B., PRZYBYLSKI M., GAWRYŚ P. 2014. *Hall effect sensor of the shaft position of the brushless DC motor*. Patent No. P218476.

WILLIAMSON S.S. 2013. *Energy Management Strategies for Electric and Plug-in Hybrid Electric Vehicles*. Springer, New York, London.